

## The oxidative dissolution of unirradiated $\text{UO}_2$ by hydrogen peroxide as a function of pH

F. Clarens<sup>a</sup>, J. de Pablo<sup>a</sup>, I. Casas<sup>a</sup>, J. Giménez<sup>a,\*</sup>, M. Rovira<sup>a</sup>, J. Merino<sup>b</sup>, E. Cera<sup>b</sup>, J. Bruno<sup>b</sup>, J. Quiñones<sup>c</sup>, A. Martínez-Esparza<sup>d</sup>

<sup>a</sup> Department of Chemical Engineering, Universitat Politècnica de Catalunya, ETSEIB, Diagonal 647 H-4, 08028 Barcelona, Spain

<sup>b</sup> Envirospan, Pg. de Rubí 29-31, 08197 Vall d'Hebron, Spain

<sup>c</sup> Ciemat, Av. Complutense 22, 28040 Madrid, Spain

<sup>d</sup> Enresa, Cl Emilio Vargas 7, 28043 Madrid, Spain

Received 29 December 2004; accepted 7 June 2005

### Abstract

The dissolution of non-irradiated  $\text{UO}_2$  was studied as a function of both pH and hydrogen peroxide concentration (simulating radiolytic generated product). At acidic pH and a relatively low hydrogen peroxide concentration ( $10^{-5} \text{ mol dm}^{-3}$ ), the  $\text{UO}_2$  dissolution rate decreases linearly with pH while at alkaline pH the dissolution rate increases linearly with pH. At higher  $\text{H}_2\text{O}_2$  concentrations ( $10^{-3} \text{ mol dm}^{-3}$ ) the dissolution rates are lower than the ones at  $10^{-5} \text{ mol dm}^{-3} \text{ H}_2\text{O}_2$ , which has been attributed to the precipitation at these conditions of studtite ( $\text{UO}_4 \cdot 4\text{H}_2\text{O}$ , which was identified by X-ray diffraction), together with the possibility of hydrogen peroxide decomposition. In the literature, spent fuel dissolution rates determined in the absence of carbonate fall in the  $\text{H}_2\text{O}_2$  concentration range  $5 \times 10^{-7}$ – $5 \times 10^{-5} \text{ mol dm}^{-3}$  according to our results, which is in agreement with  $\text{H}_2\text{O}_2$  concentrations determined in spent fuel leaching experiments.

© 2005 Elsevier B.V. All rights reserved.

PACS: 82.55; 28.41.T; 28.41.K; 82.50.G; 81.65.Mq

### 1. Introduction

The most important molecular oxidants identified in spent fuel dissolution experiments as products of the radiolysis of water are oxygen and hydrogen peroxide

[1,2]. The effect of oxygen on  $\text{UO}_2$  and spent fuel matrix corrosion has been already studied in detail using different experimental techniques [3–5]. From these dissolution studies, a semi-empirical oxidative dissolution model in the presence of oxygen has been developed [6,7], which allows us to explain experimental results at different conditions.

However, deviations of the semi-empirical model have been found when spent fuel dissolution rates have been determined at low oxygen concentrations, in which case higher dissolution rates than predicted by the model have been observed [3]. Hydrogen peroxide produced by

\* Corresponding author. Tel.: +34 93 4017388; fax: +34 93 4015814.

E-mail address: [francisco.javier.gimenez@upc.edu](mailto:francisco.javier.gimenez@upc.edu) (J. Giménez).

water radiolysis could be the responsible of these deviations. Little information about the effect of this oxidant on the spent fuel dissolution is found in literature [8–12]. In addition, hydrogen peroxide concentrations much higher than the ones expected on the surface of the fuel due to radiolysis have been often used in the studies. Hence, Bruno et al. [1,13] determined a hydrogen peroxide concentration of  $10^{-7}$  mol dm<sup>-3</sup> generated from the dissolution of 2 g of 40 MWd/KgU PWR fuel in hydrogen carbonate medium and Quiñones et al. [14] calculated a hydrogen peroxide concentration of  $10^{-6}$  mol dm<sup>-3</sup> in the absence of carbonates, while hydrogen peroxide concentrations in the range  $10^{-2}$ – $10^{-4}$  mol dm<sup>-3</sup> have been often used in the experiments.

In a previous work [15], the dissolution of UO<sub>2</sub> at different hydrogen peroxide concentrations (from  $10^{-5}$  to  $10^{-3}$  M) at constant pH 6 was studied. In those experiments both the dissolution rate (obtained from the uranium concentration measured in solution) and the oxidation rate (obtained from the decrease of the hydrogen peroxide concentration in solution) were calculated. The main conclusion was that oxidation rates were always higher than dissolution rates, indicating that the UO<sub>2</sub> surface oxidation was faster than the overall dissolution process. This conclusion was corroborated by XPS measurements of the solid surface which showed a composition of UO<sub>2.36±0.03</sub>. At more acidic pH it has been shown that the surface of the solid is not oxidized [16,17]. The same conclusion was deduced from the UO<sub>2</sub> oxidation–dissolution model developed for the results obtained in oxygen [6].

In the 1980s decade, Eary and Cathless [18] proposed a three-step mechanism for the UO<sub>2</sub> dissolution in H<sub>2</sub>O<sub>2</sub> media at acidic pH (from 1.2 to 5.5) that consisted on: (1) adsorption of the H<sub>2</sub>O<sub>2</sub> on the UO<sub>2</sub> surface; (2) oxidation of U(IV) via an electrochemical mechanism; and (3) the desorption of the products species. However, they found that at a critical pH value, the UO<sub>2</sub> surface was covered by a thin layer of uranium peroxide hydrates, which provoked the decrease of the dissolution rates. Uranium peroxide hydrates has also been reported to precipitate on spent fuel [19], on UO<sub>2</sub> irradiated by <sup>4</sup>He<sup>2+</sup> [21] and also on the surface of Chernobyl ‘lavas’ [22] and in the Shinkolobwe natural analogue [23]. In a recent paper, the precipitation of studtite on unirradiated UO<sub>2</sub> has been studied by means of the scanning force microscopy (SFM) technique in solution containing hydrogen peroxide  $5 \times 10^{-4}$  mol dm<sup>-3</sup> [20]. Recently, Burns and Hughes [24] presented the structure of the studtite while Kubatko et al. [25] determined new thermodynamic data on this solid phase.

In the present work we have studied the UO<sub>2</sub> dissolution in the presence of hydrogen peroxide at different pH values using a continuous flow-through reactor. Results are compared to those obtained by other authors with spent fuel samples.

## 2. Experimental

Dissolution experiments were carried out in a continuous flow-through reactor described elsewhere [7] using an unirradiated synthetic UO<sub>2</sub> with a particle size of 100–320 μm. The specific surface area of the solid was determined by the BET method and a value of  $0.010 \pm 0.001$  m<sup>2</sup> g<sup>-1</sup> was obtained at room temperature.

The circulation rate of the leaching solution was maintained in the range  $0.19 \pm 0.02$  cm<sup>3</sup>/min by means of a peristaltic pump. With these flow rates we ensured that steady-state conditions were achieved [17]. However, as we will describe below, this was not true in one of the experiments.

The experiments were carried out at room temperature and bubbling continuously nitrogen through the solutions in order to avoid the presence of oxygen and carbonate. The pH was monitored by means of an on-line combined glass electrode.

Uranium concentration in the outflowing solution was determined by ICP-MS (Perkin–Elmer ELAN 6000); H<sub>2</sub>O<sub>2</sub> concentration was determined by chemiluminescence using Co(II) and luminol as reagents [26].

The influence of pH on UO<sub>2</sub> dissolution rate was studied at  $10^{-5}$  mol dm<sup>-3</sup> and  $10^{-3}$  mol dm<sup>-3</sup> H<sub>2</sub>O<sub>2</sub>. In addition, the variation of the UO<sub>2</sub> dissolution rate with hydrogen peroxide concentration was studied at pH  $5.8 \pm 0.2$ .

The techniques used for the characterization of the solid phases were X-Ray Photoelectron Spectroscopy (XPS, VG Scientific Microlab MK II), Scanning Electron Microscopy (SEM, Jeol JSM-6400) and X-Ray Diffraction (XRD, Bruker D5005).

## 3. Results and discussion

The uranium concentration in solution was measured at given time intervals. Once the steady-state was reached, the dissolution rates were calculated according to the following equation:

$$r = q \cdot [U] / m \cdot S, \quad (1)$$

where  $r$  (mol m<sup>-2</sup> s<sup>-1</sup>) is the dissolution rate,  $q$  (dm<sup>3</sup> s<sup>-1</sup>) is the flow rate,  $[U]$  (mol dm<sup>-3</sup>) is the uranium concentration in solution,  $m$  (g) is the mass of UO<sub>2</sub>, and  $S$  (m<sup>2</sup> g<sup>-1</sup>) is the specific surface area of the solid. Steady-state was attained in less than 15 days.

The dissolution rates obtained at different pH values and a hydrogen peroxide concentration of  $10^{-5}$  mol dm<sup>-3</sup> are shown in Table 1 and in Fig. 1. As it can be seen the dissolution rate decreases as the pH increases, reaching a minimum between pH 7 and 9, and increases again at more alkaline pH.

Table 1  
Dissolution rates (in  $\text{mol m}^{-2} \text{s}^{-1}$ ) as a function of pH in  $10^{-5} \text{ mol dm}^{-3} \text{ H}_2\text{O}_2$

pH	Dissolution rate at $[\text{H}_2\text{O}_2] = 10^{-5} \text{ M}$
3.5	$(2.6 \pm 0.2) \times 10^{-9}$
3.6	$(1.9 \pm 0.2) \times 10^{-9}$
5	$(1.3 \pm 0.2) \times 10^{-10}$
7	$(3.6 \pm 0.4) \times 10^{-11}$
9	$(3.4 \pm 0.7) \times 10^{-11}$
10.5	$(1.0 \pm 0.1) \times 10^{-10}$

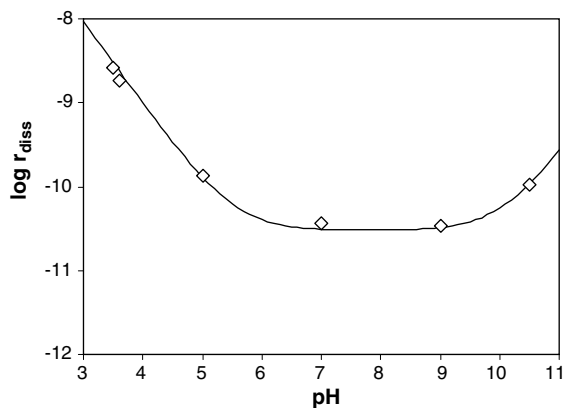


Fig. 1.  $\text{UO}_2$  dissolution rates (in  $\text{mol m}^{-2} \text{s}^{-1}$ ) as a function of pH at  $[\text{H}_2\text{O}_2] = 10^{-5} \text{ M}$ . The solid line represents the fitting of Eq. (2) with the parameters given in Table 2.

The dissolution rates as a function of pH have been fitted using an empirical model represented by the following equation:

$$r_{\text{diss}} = k_{\text{H}} \cdot [\text{H}^+]^n + k_0 + k_{\text{OH}} \cdot [\text{H}^+]^m \quad (2)$$

The fitting of this equation to the experimental dissolution rates can be also seen in Fig. 1. The values of the parameters that give the best fit are given in Table 2. A first-order dependency of the dissolution rate with respect to proton and hydroxyl anion at acidic and alkaline pH, respectively, has been found. The  $k$  values are specific of the experimental conditions under which they were determined and correspond to the hydrogen peroxide concentration,  $10^{-5} \text{ mol dm}^{-3}$ , used in these experiments.

Table 2  
Values of the parameters of Eq. (2) fitted to the experimental data at  $[\text{H}_2\text{O}_2] = 10^{-5} \text{ mol dm}^{-3}$

$k_{\text{H}}$	$8 \pm 2 \times 10^{-6}$
$k_0$	$3 \pm 1 \times 10^{-11}$
$k_{\text{OH}}$	$4.0 \pm 0.5 \times 10^{-21}$
$n$	$1.00 \pm 0.04$
$m$	$-1.00 \pm 0.04$

This empirical model is consistent with the empirical model previously developed for oxygen [5], which was later described in a more deep mechanistic way [7]. However, the side reactions present in hydrogen peroxide media [11] make at this stage much more difficult to establish an overall mechanistic approach.

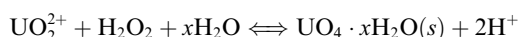
On the other hand, the  $\text{UO}_2$  dissolution rates obtained at pH 5.8 and different hydrogen peroxide concentrations can be seen in Fig. 2 and in Table 3. The dissolution rate increases linearly with the hydrogen peroxide concentration in the range  $5 \times 10^{-6}$ – $10^{-4} \text{ mol dm}^{-3}$  but seems to level off at higher  $\text{H}_2\text{O}_2$  concentration. Similar results are reported in the literature [9,10] and the comparatively low value at  $[\text{H}_2\text{O}_2] > 10^{-4} \text{ mol dm}^{-3}$  was assumed to be a consequence of the hydrogen peroxide decomposition reaction as discussed elsewhere [27,28].

We used the parameters of Eq. (2) previously determined to fit the dissolution rates obtained at pH 5.8 and at different hydrogen peroxide concentrations considering that the parameters  $k_{\text{H}}$ ,  $k_0$  and  $k_{\text{OH}}$  depend linearly with the hydrogen peroxide concentration, as deduced from previous results [15]. This fitting is shown as a solid line in Fig. 2.

As it can be seen the fitting of Eq. (2) to the experimental data is fairly good except for the value at the highest hydrogen peroxide concentration.

In order to study more accurately the behaviour of the  $\text{UO}_2$  dissolution rate at this relatively high hydrogen peroxide concentrations we carried out two different experiments at  $[\text{H}_2\text{O}_2] = 10^{-3} \text{ mol dm}^{-3}$  at pH values 3.5 and 5. The dissolution rates obtained were  $3.0 \times 10^{-10}$  and  $2.5 \times 10^{-10} \text{ mol m}^{-2} \text{s}^{-1}$ , respectively, indicating that at this relatively high hydrogen peroxide concentration the dissolution rate does not depend on pH in the acidic range.

In addition to the possibility of the existence of hydrogen peroxide decomposition at acidic to neutral pH and relatively high  $\text{H}_2\text{O}_2$  concentrations, the possible precipitation of a secondary solid phase should be considered. As we said above, a decrease of the dissolution rate at acidic pH in the presence of relatively high hydrogen peroxide concentrations was found by Eary and Cathless [18] when studying the  $\text{UO}_2$  dissolution kinetics. They found that below a critical pH value, that depended on the hydrogen peroxide concentration, the  $\text{UO}_2$  dissolution rate was independent on pH. They also examined the surface of the solid after the leaching and found that it was covered by a thin layer of uranium peroxide hydrate,  $\text{UO}_4 \cdot x\text{H}_2\text{O}$ , formed due to the following reaction:



where  $x = 2$  or  $4$  (metastudtite or studtite, respectively).

We have tested the possibility that studtite precipitated in our experiments. In the experiment with an

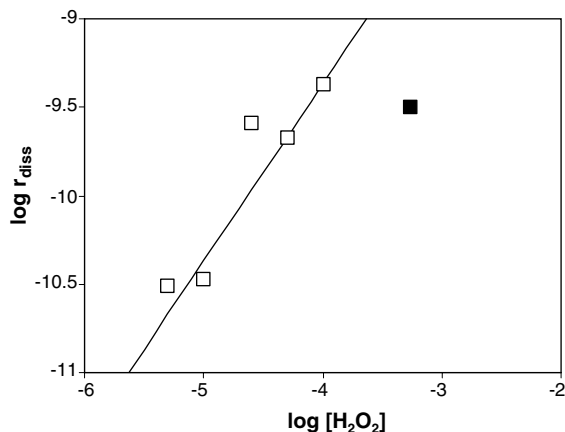


Fig. 2.  $\text{UO}_2$  dissolution rates as a function of hydrogen peroxide concentration at pH 5.8. The solid line represents the fitting of Eq. (2) to the experimental data. The black point cannot be considered as a dissolution rate because the uranium concentration in solution was not at steady-state.

Table 3

Dissolution rates (in  $\text{mol m}^{-2} \text{s}^{-1}$ ) as a function of hydrogen peroxide concentration in solution

$[\text{H}_2\text{O}_2]$ ( $\text{mol} \cdot \text{dm}^{-3}$ )	$\log r$
$5 \times 10^{-6}$	$-10.51 \pm 0.08$
$1 \times 10^{-5}$	$-10.47 \pm 0.09$
$2.5 \times 10^{-5}$	$-9.6 \pm 0.1$
$5 \times 10^{-5}$	$-9.67 \pm 0.03$
$1 \times 10^{-4}$	$-9.37 \pm 0.09$
$5.4 \times 10^{-4}$	$-9.50 \pm 0.07$

initial  $10^{-3} \text{ mol dm}^{-3} \text{ H}_2\text{O}_2$ , we measured the uranium and hydrogen peroxide concentrations in solution as well as the pH at different intervals of time, the data are presented in Table 4. With these values we have calculated the saturation index with respect to studtite considering the solubility product of this solid according to the reaction:

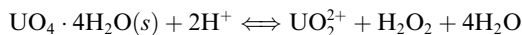


Table 4

Concentrations measured in solution in the experiment with initial  $10^{-3} \text{ mol} \cdot \text{dm}^{-3} \text{ H}_2\text{O}_2$

Time (h)	$[\text{U}]_{\text{tot}}$ (RSD = 99.1%)	$[\text{H}_2\text{O}_2]$	pH ( $\pm 0.1$ )
44.5	$5.3 \times 10^{-6}$	$(7.9 \pm 0.1) \times 10^{-4}$	3.3
112.8	$5.4 \times 10^{-7}$	$(8.7 \pm 0.1) \times 10^{-4}$	3.4
159.4	$3.2 \times 10^{-7}$	$(7.4 \pm 0.1) \times 10^{-4}$	3.4
214.1	$2.6 \times 10^{-7}$	$(9.3 \pm 0.1) \times 10^{-4}$	3.3
279.5	$4.0 \times 10^{-7}$	$(1.11 \pm 0.01) \times 10^{-3}$	3.2

given by Kubatko et al. [25];  $\log K_{s0} = -2.86$ . The saturation index has been calculated by using the following equation:

$$\text{S.I.} = \frac{Q}{K_{s0}}, \quad (3)$$

where  $Q$  has been calculated taking into account the concentrations measured in solution and the following relationship:

$$Q = \frac{[\text{UO}_2^{2+}] \cdot [\text{H}_2\text{O}_2]}{[\text{H}^+]^2} \quad (4)$$

The studtite saturation index is shown in Fig. 3 as a function of time. As it can be seen, initially the dissolution is oversaturated with respect to the studtite, tending after 7 days to a saturation index of 1 (or  $\log \text{S.I.} = 0$ , as it is shown in Fig. 3).

Due to the possibility that studtite precipitated in the experiment at these conditions (low pH and high hydrogen peroxide concentration) we increased the flow rate from  $0.19$  to  $0.3 \text{ cm}^3 \text{ min}^{-1}$  and we obtained a similar dissolution rate compared with a lower flow rate, indicating that steady-state concentrations were not reached, so we cannot actually calculate a dissolution rate (see black point in Fig. 2). At the end of the experiment, the solid was characterized by scanning electron microscopy (SEM), X-Ray photoelectron spectroscopy (XPS) and X-Ray diffraction (XRD).

The composition of the surface of the solid determined by XPS was 80% of U(IV) and 20% of U(VI) indicating that some part of the  $\text{UO}_2$  that had been oxidized did not dissolve, in contrast with the behaviour at lower hydrogen peroxide concentration. In addition, by means of SEM (see a microphotography in Fig. 4) the precipitation of a secondary phase was actually observed on the  $\text{UO}_2$  surface. This secondary phase resulted to be studtite as was determined by XRD (see Fig. 4).

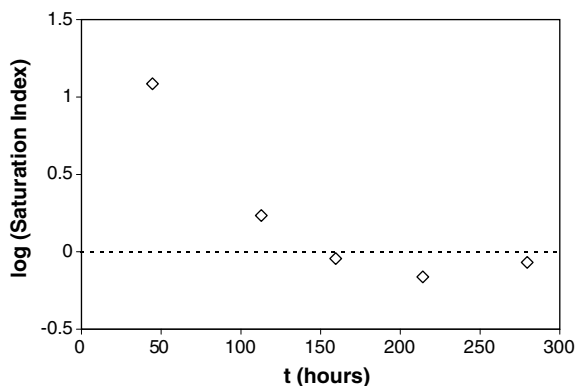


Fig. 3. Studtite saturation index as a function of time considering the concentrations measured in solution in the experiment at  $\text{pH} \approx 3$  and  $10^{-3} \text{ mol dm}^{-3}$  initial  $\text{H}_2\text{O}_2$  concentration.

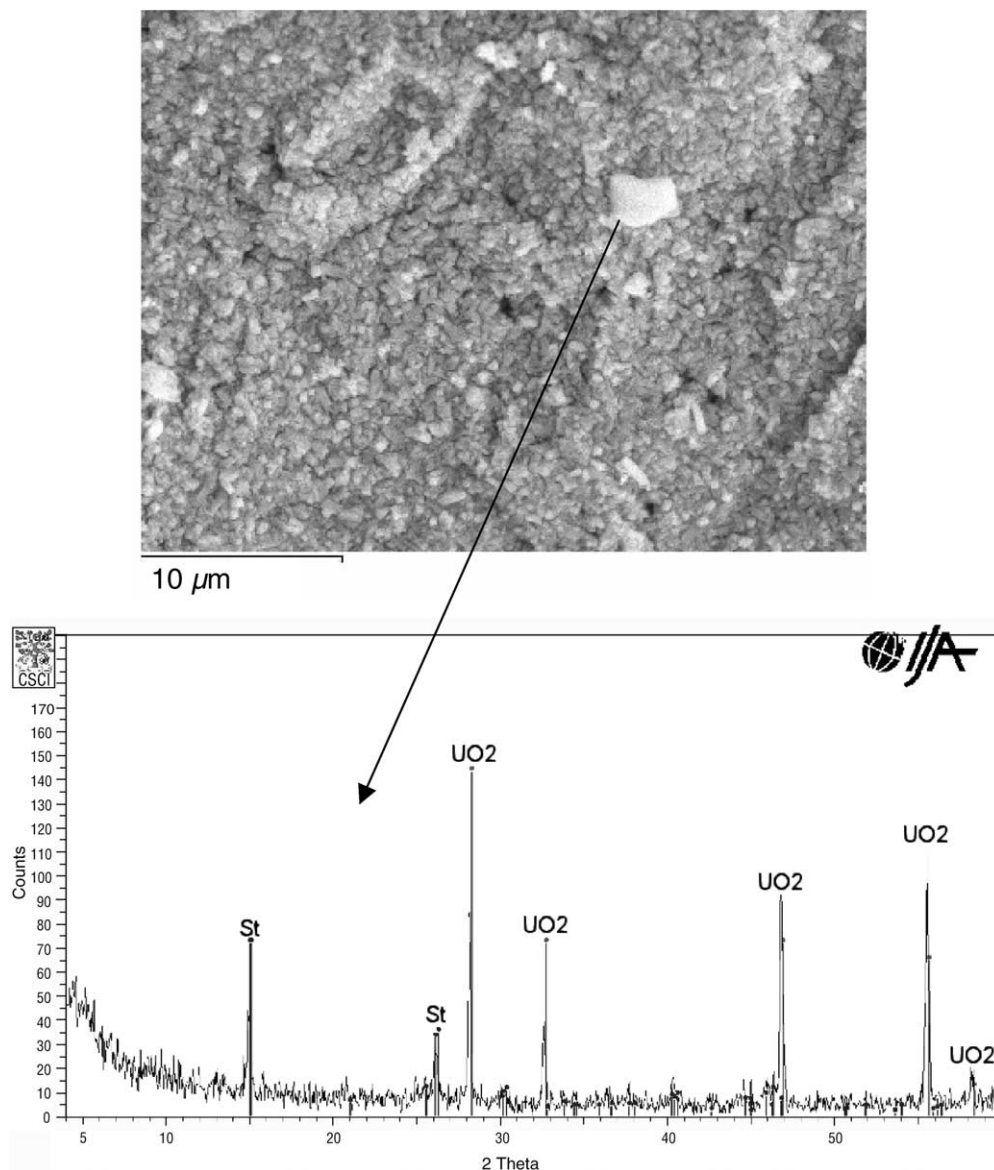
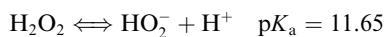


Fig. 4. Characterization of the secondary solid phase formed on the  $\text{UO}_2$  by SEM and XRD. The peaks named 'St' are the ones corresponding to studdite.

The precipitation of this secondary solid phase would explain the 'plateau' obtained in our experiments at  $10^{-3} \text{ mol dm}^{-3}$  hydrogen peroxide concentration and acidic pH.

In the alkaline pH range the behaviour of the dissolution rate is different from the one observed in the presence of  $\text{O}_2$ , where dissolution rates did not depend on pH [5,7]. The increase with pH found in  $\text{H}_2\text{O}_2$  media can be related to the increase of the decomposition of the hydrogen peroxide in alkaline media reported in the literature [29–31] and it is generally attributed to

the acidity of the hydrogen peroxide, with the following equilibrium:



Taking into account this equilibrium, the concentration of the  $\text{HO}_2^-$  at pH 10.5 would be 7% of the total hydrogen peroxide concentration. According to the literature, the perhydroxy anion would be involved in the oxidation mechanism in this pH range [29,31–33]. It is also reported that  $\text{HO}_2^-$  is a precursor of the chain of radicals that produce a stronger oxidizing environment

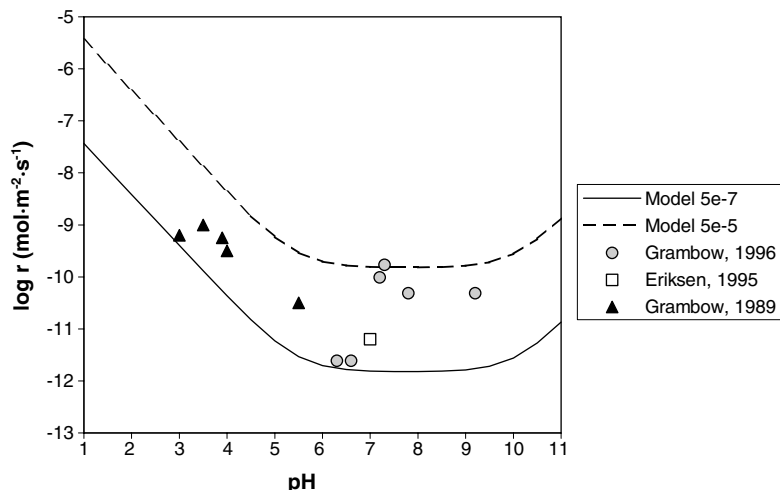


Fig. 5. Comparison of spent fuel dissolution rates with the empirical model represented by Eq. (2) at two different hydrogen peroxide concentrations.

than that of the hydrogen peroxide alone [34,35], giving an increase of the potential oxidation of the  $\text{UO}_2$  surface.

We have applied the empirical model developed in this work to some literature data on the dissolution of spent nuclear fuel in the absence of bicarbonate [1,2,36]. Fig. 5 shows the comparison between experimental data with spent fuel and the values of the model expressed by Eq. (2) at two different hydrogen peroxide concentrations. As it can be seen, without considering other oxidizing species formed due to water radiolysis, the spent fuel dissolution rates would correspond to hydrogen peroxide concentrations between  $5 \times 10^{-7}$  and  $5 \times 10^{-5} \text{ mol dm}^{-3}$ . This range includes the hydrogen peroxide concentration,  $6 \times 10^{-7} \text{ mol dm}^{-3}$ , determined by Eriksen et al. [1] in their spent fuel leaching experiments.

#### 4. Conclusions

$\text{UO}_2$  dissolution rates in the presence of hydrogen peroxide are higher than in the presence of oxygen in the pH range studied in this work (3–10.5).

At acidic pH values the dissolution rate decreases as pH increases with a first order reaction with respect to proton concentration. However at relatively high  $\text{H}_2\text{O}_2$  concentrations as well as low pH, the possibility of the precipitation of a secondary phase such as studtite has been observed.

In the alkaline range, it is observed a linear increase of the dissolution rate with pH that can be due to the presence of the perhydroxy anion,  $\text{HO}_2^-$ .

The mechanism of  $\text{UO}_2$  and spent nuclear fuel dissolution in hydrogen peroxide media seems to be more

complicated than that already developed for the oxygen. If we consider only the influence of the  $\text{H}_2\text{O}_2$  (without considering the influence of the radicals that can be formed in solution), the possible precipitation of uranium peroxides should be taken into account. In addition, in the alkaline pH range the presence of the perhydroxy anion can be crucial because it can provoke an important increase of the dissolution rate.

#### Acknowledgements

Thanks are due to Josep Elvira and Montse Marsal for the X-ray diffraction and SEM analyses, respectively. This work was financially supported by ENRESA (Empresa Nacional de Residuos, Spain), the EU (SFS project) and the Spanish 'Ministerio de Ciencia y Tecnología (MCyT)' by means of the 'Ramón y Cajal' programme.

#### References

- [1] T.E. Eriksen, U.-B. Eklund, L.O. Werme, J. Bruno, J. Nucl. Mater. 227 (1995) 76.
- [2] B. Grambow, A. Loida, P. Dressler, H. Geckeis, J. Gago, I. Casas, J. de Pablo, J. Giménez, M.E. Torrero, Chemical reaction of fabricated and high burnup spent  $\text{UO}_2$  fuel with saline brines, European Commission, Final Report EUR-17111, 1997.
- [3] W.J. Gray, C.N. Wilson, Spent fuel dissolution studies: FY 1991–1994, Report PNL-10540, USA, 1995.
- [4] D.W. Shoemith, J. Nucl. Mater. 282 (2000) 1.
- [5] M.E. Torrero, E. Baraj, J. de Pablo, J. Giménez, I. Casas, Int. J. Chem. Kinet. 29 (1997) 261.



- [6] J. de Pablo, I. Casas, J. Giménez, M. Molera, M. Rovira, L. Duro, J. Bruno, *Geochim. Cosmochim. Acta* 63 (1999) 3097.
- [7] J. de Pablo, I. Casas, J. Giménez, F. Clarens, L. Duro, J. Bruno, *Mater. Res. Soc. Symp. Proc.* 807 (2004) 83.
- [8] J.B. Hiskey, *Trans. Inst. Min. Metall. Sect. C* 89 (1980) 145.
- [9] D.W. Shoosmith, S. Sunder, *J. Nucl. Mater.* 190 (1992) 20.
- [10] J. Giménez, E. Baraj, M.E. Torrero, I. Casas, J. de Pablo, *J. Nucl. Mater.* 238 (1996) 64.
- [11] E. Ekeröth, M. Jonsson, *J. Nucl. Mater.* 322 (2003) 242.
- [12] P. Díaz-Arocas, J. Quiñones, C. Maffiotte, J. Serrano, J. García, J.R. Almazán, J. Esteban, *Mater. Res. Soc. Symp. Proc.* 353 (1995) 641.
- [13] J. Bruno, E. Cera, M. Grivé, U. Eklund, T. Eriksen, Experimental determination and chemical modelling of radiolytic processes at the spent fuel/water interface, SKB, Report TR-99-26, 1999.
- [14] J. Quiñones, J. Serrano, P. Díaz-Arocas, J.L. Rodríguez, J.A. Esteban, A. Martínez-Esparza, Influencia de la generación de productos radiolíticos en la velocidad de alteración de la matriz del combustible gastado. Parte I: Agua desionizada, CIEMAT Report DFN/RA-08/SP-99, 1999.
- [15] J. de Pablo, I. Casas, F. Clarens, F. El Aamrani, M. Rovira, *Mater. Res. Soc. Symp. Proc.* 663 (2001) 409.
- [16] S. Sunder, D.W. Shoosmith, R.J. Lemire, M.G. Bailey, G.J. Wallace, *Corrosion Sci.* 32 (1991) 373.
- [17] I. Casas, J. Giménez, V. Martí, M.E. Torrero, J. de Pablo, *Radiochim. Acta* 66&67 (1994) 23.
- [18] L.E. Eary, L.M. Cathless, *Metall. Trans. B* 14B (1983) 325.
- [19] B. McNamara, E. Buck, B. Hanson, *Mater. Res. Soc. Symp. Proc.* 757 (2003) 401.
- [20] F. Clarens, J. de Pablo, I. Díez-Pérez, I. Casas, J. Giménez, M. Rovira, *Environ. Sci. Technol.* 38 (2004) 6656.
- [21] G. Sattonnay, C. Ardois, C. Corbel, J.F. Lucchini, M.-F. Barthe, F. Garrido, D. Gosset, *J. Nucl. Mater.* 288 (2001) 11.
- [22] B.E. Burakov, E.E. Strykanova, E.B. Anderson, *Mater. Res. Soc. Symp. Proc.* 465 (1997) 1309.
- [23] J. Čejka, J. Sejkora, M. Deliens, *N. Jb. Miner. Mh.* 3 (1996) 125.
- [24] P. Burns, K.-A. Hughes, *Am. Mineral.* 88 (2003) 1165.
- [25] K.A.H. Kubatko, K.B. Helean, A. Navrotsky, P.C. Burns, *Science* 302 (2003) 1191.
- [26] D. Price, P.J. Worsfold, F.C. Montoura, *Anal. Chim. Acta* 298 (1994) 121.
- [27] D.W. Shoosmith, S. Sunder, L.H. Jonson, M.G. Bailey, *Mater. Res. Soc. Symp. Proc.* 50 (1985) 309.
- [28] S. Sunder, D.W. Shoosmith, L.H. Johnson, G.J. Wallace, M.G. Bailey, A.P. Snaglewski, *Mater. Res. Soc. Symp. Proc.* 84 (1987) 103.
- [29] J. Abbot, D.G. Brown, *Int. J. Chem. Kinet.* 22 (1990) 963.
- [30] R.J. Watts, M.K. Foget, S.-H. Kong, A.L. Teel, *J. Hazard. Mater. B* 69 (1999) 229.
- [31] I.A. Salem, R.I. Elhag, K.M.S. Khalil, *Transit. Metal Chem.* 25 (2000) 260.
- [32] R. Venkatachalapathy, G.P. Davila, J. Prakash, *Electrochem. Commun.* 1 (1999) 614.
- [33] A.H. Gemeay, *Colloid Surf. A* 116 (1996) 277.
- [34] M.A. Hasan, M.I. Zaki, L. Pasupulety, K. Kumari, *Appl. Catal. A-Gen.* 181 (1999) 171.
- [35] R. Andreozzi, V. Caprio, A. Insola, R. Martota, *Catal. Today* 53 (1999) 51.
- [36] B. Grambow, Spent fuel dissolution and oxidation. An evaluation of literature data, SKB Technical Report 89-13, 1989.